

Thermal-Vacuum Response of Polymer Matrix Composites in Space

R. C. Tennyson* and R. Matthews†

University of Toronto, Toronto, Ontario M3H 5T6, Canada

This report describes a thermal-vacuum outgassing model and test protocol for predicting outgassing times and dimensional changes for polymer matrix composites. Experimental results derived from control samples are used to provide the basis for analytical predictions to compare with the outgassing response of flight samples measured over the first 370 days in orbit on the NASA Long Duration Exposure Facility satellite. Outgassing in the space environment around this satellite is found to be much slower than in a thermal-vacuum chamber. However, the analytical model can accurately predict the dynamic outgassing response when a modified diffusion coefficient is used.

Nomenclature

D	= diffusion coefficient, mm ² /h
h	= laminate thickness, mm
M	= moisture content, %
M_0	= initial moisture content, %
Q_k	= reduced lamina stiffness matrix
T	= temperature
t	= time
x, y	= orthogonal structural axes located at laminate midplane
α	= coefficient of thermal expansion (CTE)
β	= coefficient of moisture expansion (CME)
Δ_t	= strain change at time t
ε	= strain
θ_k	= fiber orientation of k th ply, deg
1, 2	= orthogonal lamina axes corresponding to fiber and matrix directions, respectively

Introduction

FIBER-REINFORCED polymer matrix composites are used in the construction of spacecraft structures and components because of their high stiffness/weight and strength/weight ratios (compared to metals) and the fact that laminates can be designed to yield a "near-zero" CTE. One of the largest composite structures flown to date is the Canadarm—the robotic arm used on the Space Shuttle. However, polymer materials are known to outgas rapidly in vacuum, yielding primarily moisture and other constituent volatiles that can produce contamination on adjacent spacecraft components.^{1–3} In addition, such outgassing leads to dimensional changes that must be taken into account when designing a zero-distortion laminate. Dimensional changes due to outgassing are a function of temperature and laminate configuration for a given material system. Also of interest is the length of time required to reach an asymptotic state in the thermal-vacuum environment of the spacecraft. Laboratory thermal-vacuum tests are relatively easy to conduct to obtain such material response data. However, no in situ space-flight data have been published to correlate with predictions based on thermal-vacuum simulator measurements over prolonged periods of exposure.

In 1984 NASA launched the Long Duration Exposure Facility satellite (LDEF),⁴ which flew for 5.75 years in low Earth orbit prior to its retrieval in 1990. The University of Toronto Institute for

Aerospace Studies (UTIAS) provided an active composite-material experiment that consisted of a variety of graphite-, aramid-, and boron-fiber-reinforced epoxy-matrix composites located at ≈ 82 deg relative to the satellite's velocity vector. A detailed description of the UTIAS experiment can be found in Refs. 5 and 6. The following report presents results from this experiment, and from tests conducted in a thermal-vacuum chamber. Predictions of material response on LDEF are based on a Fick's-law⁷ model analysis outlined below.

Analysis of Moisture Desorption and Dimensional Change

As in many other published analyses, the moisture desorption M can be estimated using Fick's law from the equation (see, for example, Ref. 7)

$$M(t)_{T=\text{const}} \approx M_0 \exp \left[-7.3 \left(\frac{Dt}{h^2} \right)^{0.75} \right] \quad (1)$$

For constant temperature, Shen and Springer¹ have shown that the diffusion coefficient can be calculated knowing the moisture content at different times from the relation

$$D_{T=\text{const}} = \frac{\pi h^2}{16M_0^2} \left(\frac{M_2 - M_1}{\sqrt{t_2} - \sqrt{t_1}} \right)^2 \quad (2)$$

where M_1 and M_2 are the moisture contents at times t_1 and t_2 , respectively.

Rather than measure moisture content during a test, one can employ strain data (ε). Noting that

$$\varepsilon = M\beta \quad (3)$$

Eqs. (1) and (2) can be rewritten as

$$\varepsilon(t)_{T=\text{const}} \approx \varepsilon_0 \exp \left[-7.3 \left(\frac{Dt}{h^2} \right)^{0.75} \right] \quad (4)$$

$$D(t)_{T=\text{const}} = \frac{\pi h^2}{16\varepsilon_0^2} \left(\frac{\varepsilon_2 - \varepsilon_1}{\sqrt{t_2} - \sqrt{t_1}} \right)^2 \quad (5)$$

To develop a model for predicting outgassing of materials in space, it is necessary to take temperature into account. However, Fick's law as previously described applies to constant-temperature, constant-humidity environments. In space, the humidity is constant (zero).

Received Jan. 19, 1994; revision received July 14, 1994; accepted for publication July 28, 1994. Copyright © 1994 by the American Institute of Aeronautics and Astronautics, Inc. All rights reserved.

*Professor and Director, Institute for Aerospace Studies, 4925 Dufferin Street, North York.

†Research Associate, Institute for Aerospace Studies, 4925 Dufferin Street, North York.

Furthermore it is possible to determine a diffusion coefficient as a function of temperature $[D(T)]$ by performing outgassing tests at different temperatures (T_a and T_b) assuming an Arrhenius relation between D and T . This yields the equation

$$D(T) = \exp\left(\frac{\ln D_b - \ln D_a}{1 - (T_a/T_b)} + \ln D_a\right) \exp\left(\frac{\ln D_b - \ln D_a}{((1/T_a) - (1/T_b))T}\right) \quad (6)$$

This equation can be used to calculate the diffusion coefficient at any temperature, as long as the diffusion coefficients D_a and D_b at temperatures T_a and T_b are known. All of the above temperatures must be absolute (K).

Hence, knowing $D(T)$, the strain $\varepsilon(T, t)$ associated with outgassing can be calculated from Eq. (4).

Laminate Analysis

Consider an N -ply laminate characterized by a set of lamina properties defined by

$$\phi_l = \begin{bmatrix} \phi_1 \\ \phi_2 \\ 0 \end{bmatrix} \quad (7)$$

where ϕ_1 and ϕ_2 correspond to the fiber and transverse properties, respectively. Examples of ϕ_l include both coefficient of thermal expansion (CTE) and coefficient of moisture expansion (CME),

$$\phi_l = \alpha_l = \begin{bmatrix} \alpha_1 \\ \alpha_2 \\ 0 \end{bmatrix} \quad (\text{CTE}) \quad \text{and} \quad \phi_l = \beta_l = \begin{bmatrix} \beta_1 \\ \beta_2 \\ 0 \end{bmatrix} \quad (\text{CME}) \quad (8)$$

where $\alpha = \varepsilon/\Delta T$ and $\beta = \varepsilon/\Delta M$. For an N -ply laminate consisting of a set of plies $k = 1$ to N having arbitrary orientations θ_k and stacking sequence, the structural properties defined by ϕ_S can be calculated from the following matrix equation⁸:

$$\begin{bmatrix} \phi_S \\ \kappa \end{bmatrix} = \begin{bmatrix} A & B \\ B & D \end{bmatrix}^{-1} \begin{bmatrix} J \\ H \end{bmatrix} \begin{bmatrix} \phi_1 \\ \phi_2 \\ 0 \end{bmatrix} \quad (9)$$

where

$$\phi_S = \begin{bmatrix} \phi_x \\ \phi_y \\ \phi_{xy} \end{bmatrix}, \quad \kappa = \begin{bmatrix} \kappa_x \\ \kappa_y \\ \kappa_{xy} \end{bmatrix}$$

are the laminate curvatures,

$$\begin{bmatrix} A & B \\ B & D \end{bmatrix}^{-1}$$

is the inverse of the standard laminate stiffness matrix,⁸

$$J = \sum_{k=1}^N \tilde{T}_k^{-1} \cdot Q_k (h_k - h_{k-1}) \quad \text{and} \quad H = \sum_{k=1}^N \frac{1}{2} \tilde{T}_k^{-1} \cdot Q_k (h_k^2 - h_{k-1}^2) \quad (10)$$

$$\tilde{T} = \begin{bmatrix} m^2 & n^2 & 2mn \\ n^2 & m^2 & -2mn \\ -mn & mn & m^2 - n^2 \end{bmatrix}$$

is the transformation matrix, Q_k is the reduced lamina stiffness matrix for the k th ply,⁸

$$m = \cos \theta, \quad n = \sin \theta$$

θ is the ply angle, and h_k is the thickness of the k th ply.

Composite Material Response on LDEF

Selected composite material tubular samples were instrumented with conventional foil resistance strain (MM-WK-13-250 BG-350) and temperature (MM-STG-50C) gauges.⁶ These gauges were sampled every 16 h over the first 370 days in orbit.

Data were stored on a magnetic tape cassette using a space-qualified data acquisition system designed and constructed at UTIAS. Details on this aspect of our experiment can be obtained from Ref. 6. It was found that the strain/thermal-gauge measuring system worked flawlessly, as evidenced by the measured response of a stainless steel calibration specimen, which remained unchanged throughout the 5.75 y in orbit. Typical time temperature and strain temperature data for one material (graphite/epoxy, 5208/T300) are shown in Figs. 1 and 2, respectively. These data can be replotted as strain vs temperature as given in Fig. 3 for the 90-deg laminate. It can be seen that a "total" dimensional strain change of $\approx 1600 \times 10^{-6}$ occurred after about 80 days in orbit. It should be noted that no microcracks were observed in this laminate and full recovery of the dimensional change resulted once the sample was returned to Earth and exposed to the ambient environment.

From these data, it is possible to estimate the CTE from the final slope once all outgassing is essentially finished. Using this CTE value, one can correct for the temperature variations on-orbit, giving the strain change of the sample, over time, independent of temperature. The formula used to do this is

$$\Delta_t = \varepsilon_t - (T_t - T_{\text{Ref}})\alpha \quad (11)$$

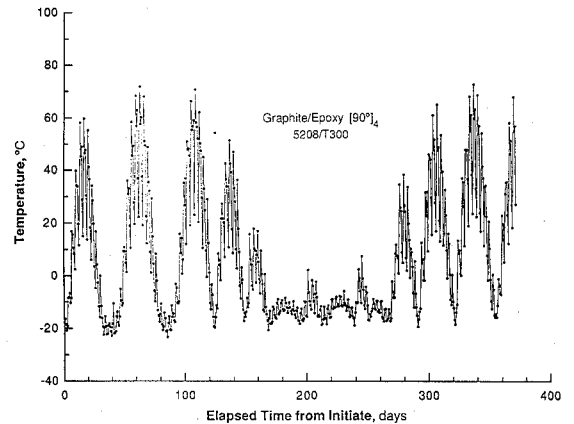


Fig. 1 Thermal history of LDEF specimen (3T6).

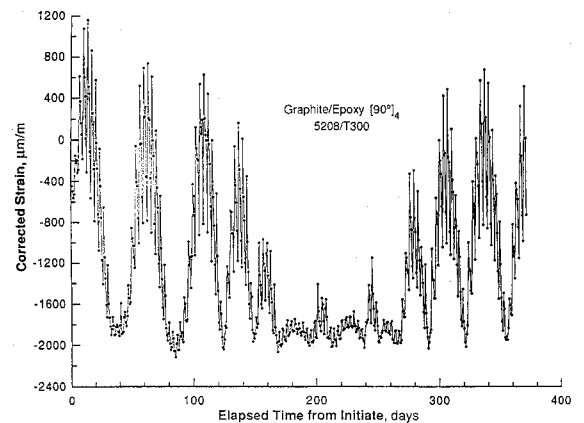


Fig. 2 Strain-time history of LDEF specimen (3T6).

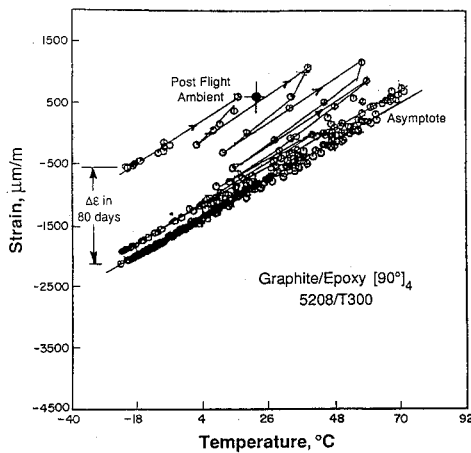


Fig. 3 Thermal strain response of LDEF specimen (3T6), graphite/epoxy [90 deg]₄ 5208/T300.

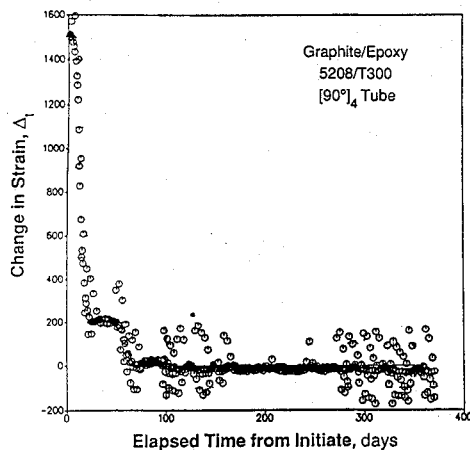


Fig. 4 Strain change vs time in orbit for LDEF specimen (3T6).

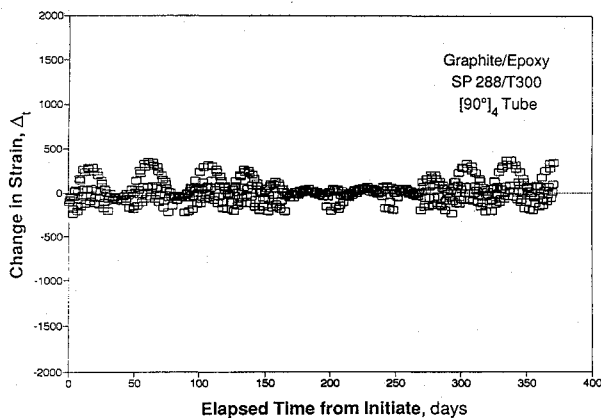


Fig. 5 Strain change measured in fiber direction (0 deg) vs time in orbit for LDEF specimen.

where $\Delta\epsilon$ is the strain change at time t ; ϵ_t is the measured strain at time t ; T_t is the temperature at time t ; T_{Ref} is the reference temperature, 24°C; and α is the CTE of the material.

The change $\Delta\epsilon$ was then plotted against time, and an adjustment factor $\Delta\epsilon_{adj}$ was added to every point. This had the effect of shifting the graph so that the final strain was zero, allowing the total strain change to be read easily. Figure 4 shows the adjusted $\Delta\epsilon_{adj}$ -vs-time curve for a 90-deg graphite/epoxy laminate (5208/T300). From this graph it is evident that outgassing was completed in about 80–100 days. It is clear that outgassing was very rapid over the first 25 days, then slowed because of the low temperatures encountered (see Fig. 1). Outgassing then increased after 50 days as the sample

temperature increased, and eventually no significant dimensional change occurred after about 80–100 days exposure. Similar behavior was exhibited by the other composite materials.^{5,6} It is interesting to note that in the fiber direction (i.e., at 0 deg), very small changes $\Delta\epsilon$ were observed, as illustrated in Fig. 5 for another graphite/epoxy material (SP288/T300). In general, the outgassing time required to reach an equilibrium state in space depends on such factors as the initial moisture concentration, volatile content, laminate thickness, ambient temperature, and constituent material diffusion properties.

Ground-Based Thermal-Vacuum Tests: Thermal-Vacuum Facility with Laser Interferometer

A standard vacuum system consisting of a stainless steel chamber, a mechanical roughing pump, and a diffusion pump was assembled to provide a vacuum environment of $\sim 10^{-6}$ Torr. Heating of the composite samples was achieved using a 50-W electrical resistance system. Copper cooling coils fed with liquid nitrogen were sufficient to achieve the low temperatures encountered by the specimens on LDEF. Both the heating and cooling cycles were controlled electronically with solenoid valves and relays. Utilizing type T thermocouples bonded to the samples, in conjunction with an amplifier system for processing the thermocouple signals, together with a cold-junction reference, permitted temperature readings to an accuracy of $\pm 1^\circ\text{C}$. Because of the small strains associated with the low-distortion laminates, a laser interferometry system was incorporated into the chamber design. A helium-neon laser provided the beam, which was split into a reference signal and a component that was reflected off one end of the sample tube fitted with a quartz mirror. Distortion of the tube, either due to thermal changes or outgassing, was measured from the resulting interference fringe patterns. As the tube distorts, the fringes move, as detected by a bicell photodetector. An electronic fringe counter was designed and constructed to record the distortion. The accuracy of this system was equivalent to a 316-nm dimensional change. The sample ends were flat and parallel to ± 0.025 mm, and the movement of the mirror was constrained to keep it vertical so as to avoid unstable fringe motion over time.

All signals emanating from the laser-interferometer-thermal-vacuum system were processed by a specially designed interface unit connected to a PC. Using custom software, all system functions were automated to provide continuous unattended usage with the data stored continuously on disk.

Experimental Procedures and Results

The following test protocol was established utilizing LDEF "control" and "flight" samples. It should be noted that all control specimens were made at the same time from the same material batch as the flight articles, and stored at ambient laboratory conditions.

1) Samples were subjected to vacuum outgassing at elevated temperature to obtain their dry-weight values.

2) For given temperature T and relative humidity, moisture uptake (in percent) was recorded for a given material from its "dry" state as a function of time t to saturation. Figure 6 shows moisture absorption data for several LDEF flight and control specimens (see Table 1).

3) The sample strain ϵ was measured as a function of time t in vacuum for two temperatures (T_a and T_b). Both experiments employed samples having the same M_0 .

Figures 7 and 8 present initial outgassing data at temperatures of 22 and 50°C for control (5T5) and flight (2T13) samples, respectively. The strain response was measured in situ using laser interferometry.

Prior to analyzing the LDEF data in detail, two issues regarding material response and the measuring systems warrant some discussion. The LDEF flight samples were monitored using bonded surface strain gauges, whereas the laboratory tests were conducted using laser interferometry. A comparison of the two system responses, based on the test of a flight sample in the vacuum chamber, is shown in Fig. 9, where it is evident that excellent correlation exists. The question of whether Fick's law is a good model for the

Table 1 Comparison of flight and control sample diffusion coefficients for $[90^\circ]_4$ graphite/epoxy laminates (5208/T300) as measured in vacuum chamber

Sample no.	Status	Temp., °C	M_i , %	$\Delta\epsilon$, 10^{-6}	CME, $10^{-6}/\%$	D, mm^2/h
5T5	Control	22	0.490	-1200	2449	0.00010
5T5	Control	50	0.550	-1939	3525	0.00047
2T13	Flight	22	0.505	-1212	2400	0.00013
2T13	Flight	22	0.510	-1224	2400	0.00008
2T13	Flight	50	0.632	-1517	2400	0.00078
3T6	Flight	22	0.500	-1200	2400	0.00014
3T6	Flight	22	0.510	-1219	2400	0.00009

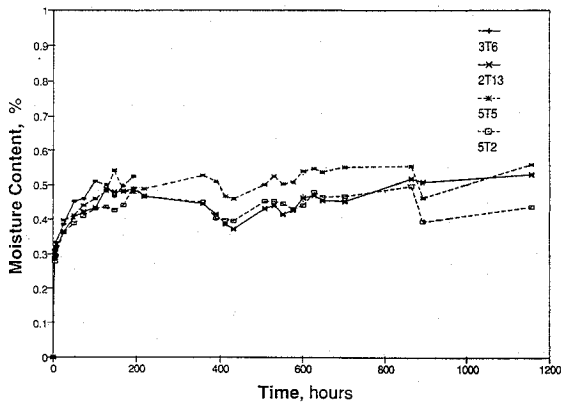


Fig. 6 Moisture absorption response of LDEF samples at 50°C and 75% relative humidity.

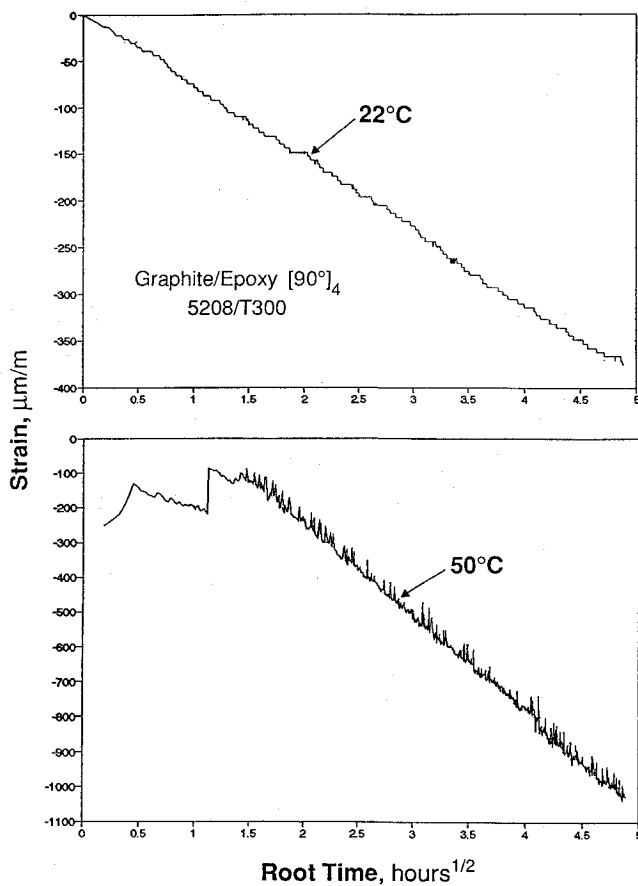


Fig. 7 Outgassing test on control specimen (5T5).

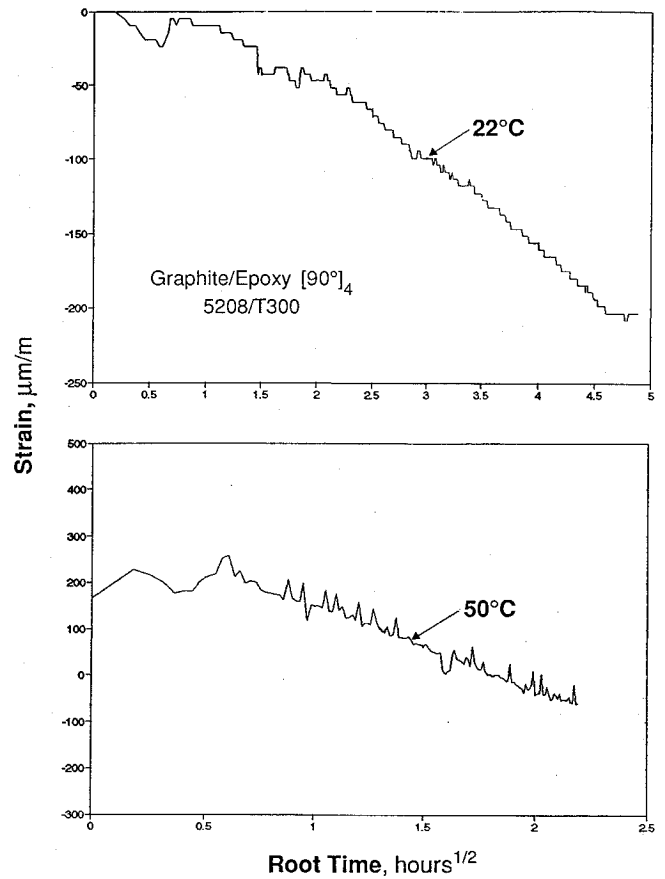


Fig. 8 Outgassing test on LDEF flight specimen (2T13).

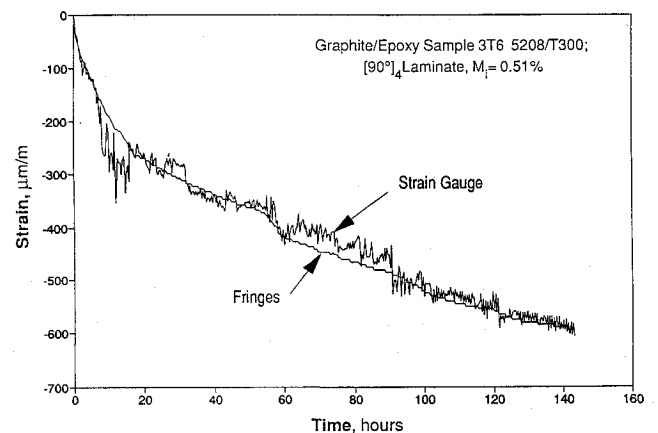


Fig. 9 Comparison of outgassing response measured by strain-gauge and laser interferometry.

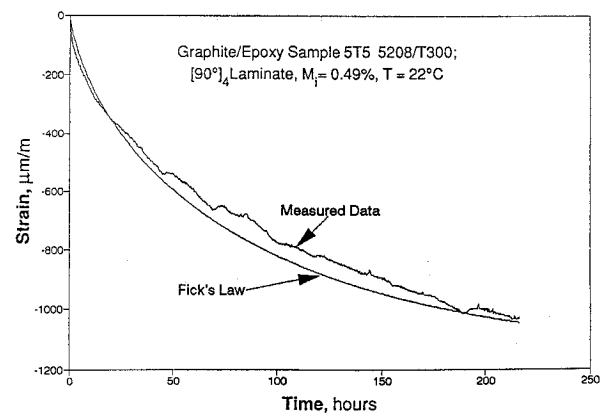


Fig. 10 Comparison of outgassing response with Fick's-law prediction.

graphite/epoxy composite material is addressed in Fig. 10. Using a control sample that was vacuum-dried and saturated to 0.49% moisture content, then allowed to outgas at $T = 22^\circ\text{C}$, provided the $\varepsilon(t)$ curve shown. Employing the previous analysis to estimate the diffusion coefficient D , the Fick's-law prediction was compared with the measured long-term response. Reasonable agreement was obtained. Thus one can proceed with confidence in the analytical model and test procedures.

Comparison with LDEF Data Calculation Procedures Using Thermal-Vacuum Test Curves

The procedure is as follows:

1) Using the $\varepsilon(T, t)$ curves, calculate the initial slope from Eq. (5) to obtain $D_a(T_a)$ and $D_b(T_b)$.

2) Determine $D(T)$ from Eq. (6) based on $D_a(T_a)$, $D_b(T_b)$, T_a , and T_b . Table 1 summarizes the values obtained for $D(T)$ for both flight and control samples of graphite/epoxy [90 deg]₄ laminates (5208/T300).

3) Using the LDEF temperature time profile obtained in orbit (Fig. 1), calculate the dynamic strain change $\varepsilon(t)$ for given time steps Δt , using the above $D(T)$ equation evaluated at the appropriate temperature. The function $\varepsilon(t)$ is given by

$$\varepsilon_t = \varepsilon_{t-1} - \varepsilon_{t-1} \left\{ 1 - \exp \left[-7.3 \left(\frac{D(\bar{T}_t) \Delta t}{h^2} \right)^{0.75} \right] \right\} \quad (12)$$

where \bar{T}_t is the average temperature over Δt , assuming ε_0 is known at $t = 0$ from the outgassing test. By using this equation at every time step over the temperature history, it is possible to calculate the strain change of the sample due to outgassing, taking into account temperature effects.

From the outgassing response shown in Fig. 4, it is evident that the moisture diffusion process essentially ceases when the temperature drops to freezing or below (i.e., $D \approx 0$ when $T \leq 0^\circ\text{C}$). This constraint can then be included in the $\varepsilon(t)$ prediction.

Comparison with LDEF Data

Based on the data in Table 1, values $D_a \approx 0.00013 \text{ mm}^2/\text{h}$ and $D_b \approx 0.00078 \text{ mm}^2/\text{h}$ were selected, corresponding to temperatures of 22 and 50°C , respectively. Using these results in Eq. (6) together with the temperature time profile shown in Fig. 1, the predicted dimensional change for the graphite/epoxy 90-deg laminate (5208/T300) is plotted in Fig. 11 together with the measured LDEF response as a function of time in orbit. Curve 1 represents the case when no correction is applied for $T \leq 0^\circ\text{C}$. One can see the effect of assuming zero outgassing of moisture exhibited by curve 2. Although the initial response prediction agrees well with flight data, it is clear that the predicted times to complete outgassing differ significantly from the flight measurements.

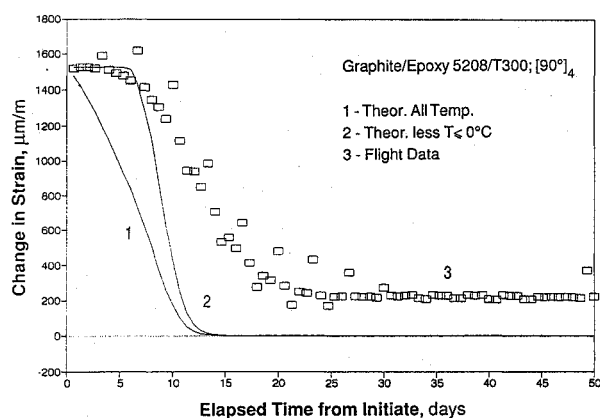


Fig. 11 Comparison of predicted outgassing response with LDEF flight sample.

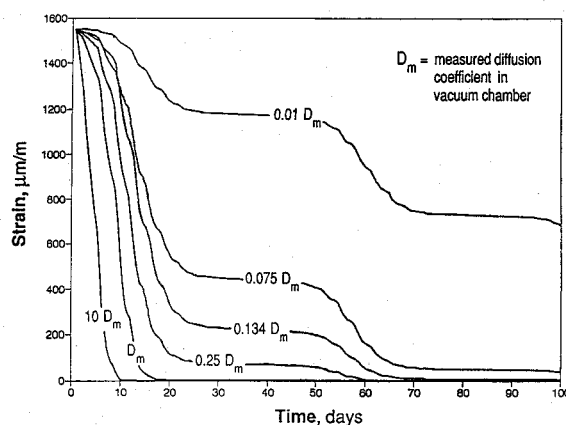


Fig. 12 LDEF outgassing predictions for T300/5208 [90 deg]₄ laminate.

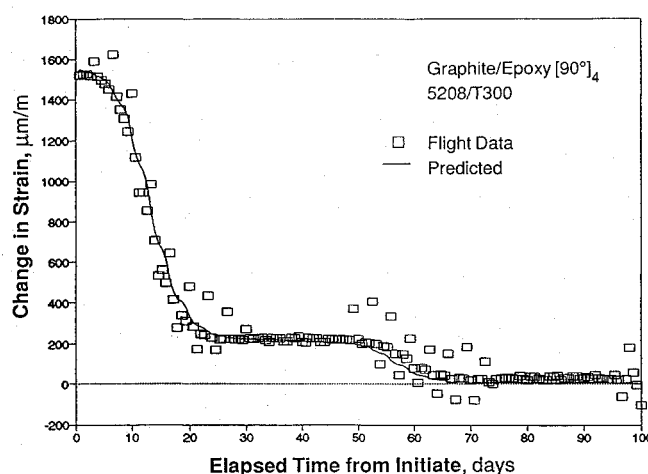


Fig. 13 Comparison of corrected prediction of strain/time response in space with LDEF flight specimen ($D^* = 0.134D_m$).

Theoretical predictions were then made for various values of the diffusion coefficient, and the dimensional changes plotted in Fig. 12. Using these results, one can see in Fig. 13 that for a diffusion coefficient of $D^* \approx 0.134D_m$ (where D_m is the measured value in the vacuum chamber), excellent agreement with the flight data is obtained. Thus the theoretical model is quite capable of predicting the outgassing dimensional changes once the appropriate diffusion coefficient is known, even over the complete thermal cycling environment.

Why is there such a difference in the diffusion coefficients measured in space and in the vacuum chamber? The tests reported show good correlation between control and flight samples. Moisture saturation and uniform distribution through the laminate was achieved. In addition, the two measuring systems correlate very well. The only explanation we have to offer is the possible effect of surface contamination of the LDEF flight samples in the early stages of deployment. Over time, this contamination was removed from the samples by atomic oxygen. Hence, when the flight samples were tested in the vacuum chamber, no contamination effects were observed. This may account for the apparent increase in outgassing time observed in orbit.

Coefficient of Thermal Expansion

As discussed earlier, after outgassing is essentially completed, one finds the thermal-strain response asymptotes, as can be seen in Fig. 3 for the [90 deg]₄ graphite/epoxy material (5208/T300). This behavior was typical of all our LDEF samples (see Ref. 1 for example). Table 2 summarizes the slope values of these curves (i.e., the CTE) for a variety of materials studied. The "ambient"

Table 2 Comparison of CTE data from LDEF experiment

Sample	Material	Laminate type	Ambient CTE, $10^{-6}/^{\circ}\text{C}$	Space CTE, $10^{-6}/^{\circ}\text{C}$	Postflight ^a CTE, $10^{-6}/^{\circ}\text{C}$
Control	T300/5208	(90 deg) ₄	—	—	24.5
Flight	T300/5208	(90 deg) ₄	—	—	24.7
Flight	T300/5208	(90 deg) ₄	28.1	28.9	—
Control	T300/5208	(± 45 deg) _s	—	—	1.93
Flight	T300/5208	(± 45 deg) _s	—	—	-6.53
Flight	T300/934	(90 deg) ₄	26.5	27.3	—
Flight	T300/SP-288	(90 deg) ₄	26.3	26.8	—
Flight	SP-290	(± 30 deg) _s	2.8	2.21	—
	Boron/epoxy	(± 60 deg) _s	21.1	20.9	—
Flight	SP-328	(90 deg) ₄	61.0	59.2	—
	Kevlar/epoxy	(0 deg) ₄	0.18	0.83	—
Control	SP-328	(± 45 deg) _s	—	—	-0.04
Flight	SP-328	(± 45 deg) _s	—	—	2.52

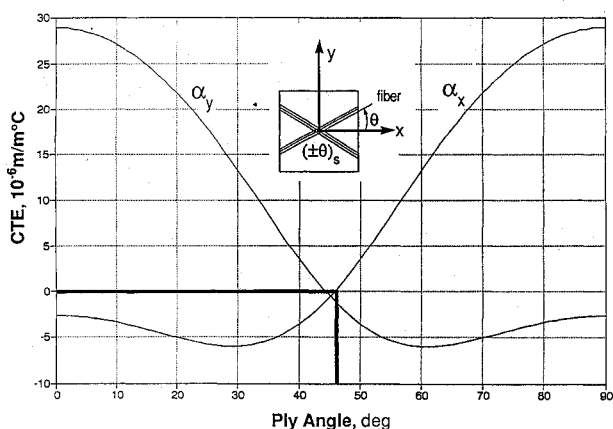
^aMeasured after complete vacuum outgassing.

Fig. 14 CTE for angle-ply T300/5208 graphite/epoxy laminates.

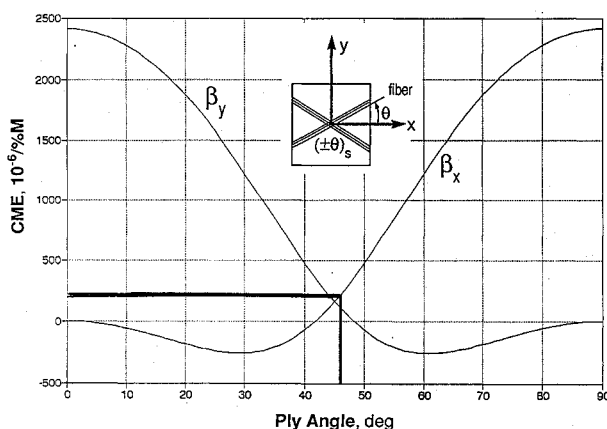


Fig. 15 CME for angle-ply T300/5208 graphite/epoxy laminates.

values represent preflight measurements, which compare in most instances reasonably well with the final asymptotic slopes obtained from the actual flight data. Some postflight CTE results are also presented, based on laser interferometer measurements after complete outgassing had occurred.

Application to Design

To demonstrate how these diffusion data and analysis can be used in the design of low-distortion laminates, consider the case of a ($\pm\theta$)_s structure. The question being addressed is how much

axial distortion can occur in a zero-CTE laminate due to vacuum outgassing.

Figure 14 presents the variation in the CTE values α_x and α_y for a ($\pm\theta$)_s laminate fabricated from 5208/T300 material. The curves shown were determined using Eq. (9). The case of $\alpha_x=0$ occurs when $\theta \approx \pm 46$ deg. Using diffusion data to calculate the CME values β_x and β_y from Eq. (9), one can obtain from Fig. 15 a value $\beta_x \approx 200 \times 10^{-6}/\%$ at $\theta = 46$ deg.

Assuming a 1% moisture uptake prior to launch yields an axial displacement of $\Delta L = 200 \times 10^{-6}L$, where L is the length of the structure. Thus for a 10-m-long structure, the axial contraction would be 2.0 mm for a zero-CTE laminate.

Summary

This report presents thermal-vacuum outgassing results for polymer matrix composites based on in situ measurements made on space-flight samples and ground-based tests. Using the laboratory data together with a Fick's-law model analysis, predictions of the dimensional changes as a function of temperature and time in the space environment were compared with flight measurements.

It was found that outgassing of the LDEF polymer matrix composites took much longer to asymptote in orbit than in a thermal-vacuum chamber. It is postulated that outgassing caused surface contamination of the LDEF samples, thus inhibiting the diffusion process. The surface contaminants were then removed over time by the incident atomic oxygen, which proceeded to erode the composite material as well. However, it was demonstrated that the analytical model was capable of reproducing the LDEF flight sample response extremely well once a modified diffusion coefficient was used. In addition, it was observed that the asymptotic thermal strain response of the flight samples yielded CTE values close to their original ambient measurements.

Acknowledgments

This research was sponsored by the Canadian Space Agency (CSA) under Contract 025SR.9F009-1-1435 and two Ontario Centres of Excellence: the Institute for Space and Terrestrial Science and the Ontario Centre for Materials Research. Special thanks are extended to D. G. Zimcik of the CSA for his continued support of our work.

References

- Shen, C., and Springer, G. S., "Moisture Absorption and Desorption of Composite Materials," *Journal of Composite Materials*, Vol. 10, Jan. 1976, pp. 2-20.
- Shirrell, C. D., and Halpin, J., "Moisture Absorption and Desorption in Epoxy Composite Laminates," *Composite Materials: Testing and Design (Fourth Conference)*, ASTM STP 617, 1977, pp. 514-528.

³Whitney, J. M., and Browning, C. E., "Some Anomalies Associated with Moisture Diffusion in Epoxy Matrix Composite Materials," *Advanced Composite Materials—Environmental Effects*, edited by J. R. Vinson, ASTM STP 658, 1978, pp. 43–60.

⁴Levine, A. S. (ed.), "LDEF—69 Months in Space," NASA CP 3134, June 1991.

⁵Tennyson, R. C., "Composite Materials in Space—Results from the LDEF Satellite," *Journal of the Canadian Aeronautics and Space Institute*, Vol. 37, No. 3, 1991, pp. 120–133.

⁶Tennyson, R. C., Mabson, G. E., Morison, W. D., and Kleiman, J., "Space

Environmental Effects on Polymer Matrix Composites—The UTIAS/LDEF Experiment," *Proceedings on Materials in a Space Environment*, Cépadués-Editions, Toulouse, France, Sept. 1991, pp. 93–110.

⁷Crank, J., and Park, G. S., *Diffusion in Polymers*, Academic, London, 1968, p. 452.

⁸Halpin, J. C., *Primer on Composite Materials: Analysis*, revised ed., Technomic, 1984, p. 187.

R. K. Clark
Associate Editor